Chemosphere 263 (2021) 128239

Contents lists available at ScienceDirect

Chemosphere

journal homepage: www.elsevier.com/locate/chemosphere

Characterization of organic aerosols in PM_1 and their cytotoxicity in an urban roadside area in Hong Kong

Xinyi Niu [a, b, 1], Yichen Wang [c, 1], Steven Sai Hang Ho [d, e], Hsiao-Chi Chuang [f], Jian Sun [g], Linli Qu [e], Gehui Wang [h], Kin Fai Ho [a, *]

[a] The Jockey Club School of Public Health and Primary Care, The Chinese University of Hong Kong, Hong Kong, China
[b] School of Human Settlements and Civil Engineering, Xi'an Jiaotong University, Xi'an, Shaanxi, 710049, China
[c] School of Humanities, Economics and Law, Northwestern Polytechnical University, Xi'an, 710129, China
[d] Division of Atmospheric Sciences, Desert Research Institute, Reno, NV, 89512, United States
[e] Hong Kong Premium Services and Research Laboratory, Hong Kong, China
[f] School of Respiratory Therapy, College of Medicine, Taipei Medical University, Taipei, Taiwan
[g] Department of Environmental Science and Engineering, Xi'an Jiaotong University, Xi'an, Shaanxi, 710049, China
[h] Key Lab of Geographic Information Science of the Ministry of Education, School of Geographic Sciences, East China Normal University, Shanghai, 210062, China

HIGHLIGHTS

- Organics composed 55% of NR-PM_1 followed by sulfate, ammonium, nitrate and chloride.
- Primary OA, more-oxidized and less-oxidized oxygenated OA were major organic sources.
- Traffic and cooking emissions were dominant pollution sources in the roadside station.
- Oxidative and inflammatory responses were occurred after exposure to PM_1 samples.
- Primary organic compounds from traffic and cooking were critical in PM-induced cytotoxicity.

GRAPHICAL ABSTRACT

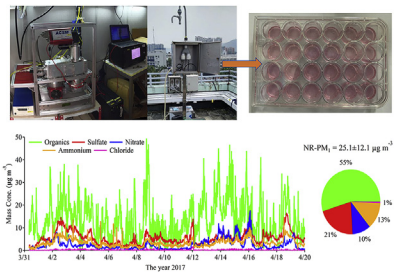

ARTICLE INFO

Article history:
Received 4 July 2020
Received in revised form
18 August 2020
Accepted 31 August 2020
Available online 3 September 2020

Handling Editor: Jianying Hu

Keywords:
Aerosol chemical speciation monitor
Organic compounds

ABSTRACT

Organic compounds in fine particles play major roles in cardiopulmonary diseases. A study was conducted to determine the characteristics and cytotoxicity of organic aerosols (OA) in an urban roadside area in Hong Kong. Chemical components in nonrefractory submicron aerosol (NR-PM_1) were observed using a Quadrupole Aerosol Chemical Speciation Monitor (Q-ACSM), and the chemical profile of organic compounds in NR-PM_1 was examined with filter-based approach. Associations between cytotoxicity and organic sources and compositions were evaluated. NR-PM_1 contributed to 84% of the PM_1 concentrations. The NR-PM_1 was composed of organics (55 ± 15%), followed by sulfate (21 ± 9%), ammonium (13 ± 6%), nitrate (10 ± 6%) and chloride (1 ± 1%). Three major organic sources were identified using positive matrix factorization, namely primary organic aerosol (POA, 40 ± 19%), more-oxidized oxygenated OA (MO-OOA, 32 ± 22%) and less-oxidized oxygenated OA (LO-OOA, 28 ± 19%). Variations in organic groups, including alkanes, hopanes, steranes, polycyclic aromatic hydrocarbons (PAHs), oxy-PAHs (OPAHs), and fatty acids, demonstrated that traffic and cooking emissions were dominant pollution sources in this roadside

* Corresponding author.
E-mail address: kfho@cuhk.edu.hk (K.F. Ho).
[1] These authors contributed equally to the study.

https://doi.org/10.1016/j.chemosphere.2020.128239

Oxidative stress
Inflammation

station. Human lung alveolar epithelial (A549) cells were exposed to PM_1, revealing increases in lactate dehydrogenase (LDH), reactive oxygen species (ROS), and interlukin-6 (IL-6), which indicated the occurrence of inflammatory and oxidative responses. POA was significantly associated with ROS and IL-6, and alkanes, hopanes, steranes, PAHs and OPAHs, and fatty acids presented medium to high correlations with LDH and IL-6, demonstrating the importance of primary emissions and organic compounds in cytotoxicity. This study demonstrated that organic compounds emitted from traffic and cooking play critical roles in PM-induced oxidative stress and inflammation in urban areas.

1. Introduction

Long-term exposure to particulate matter (PM) has been well-recognized as a critical potential factor for cardiopulmonary system diseases (Feng et al., 2016). Short-term exposure can exacerbate respiratory diseases, including airway inflammation, bronchitis and asthma, lung function decline and chronic obstructive pulmonary disease (Jia et al., 2017; Kim et al., 2015; Oh et al., 2011; Riva et al., 2011). The size, composition, and source of PM and their interaction are responsible for PM's adverse health effects (Abbas et al., 2019; Perrone et al., 2013). Organic matter, a major chemical component of PM, has been regarded as a dominant driver of cytotoxic effects induced by PM (Lui et al., 2016; Ovrevik et al., 2010). Hence, toxicological studies on organic aerosols (OAs) are required to obtain more information on the roles of different OA components and their sources.

Associations between PM exposure and pulmonary health effects have been widely studied, and the components of PM have diverse effects because of their different chemical properties (Lin et al., 2016). OAs, which consist of various individual organic compounds, account for over one-third of the mass of $PM_{2.5}$ (PM with aerodynamic diameter less than 2.5 μm) (Sun et al., 2013). Primary OAs (POAs) are emitted directly from pollution sources, including vehicles and cooking emissions, coal combustion, and biomass burning (Zhang et al., 2009). Secondary OAs (SOAs) are formed through atmospheric photochemical reactions that frequently occur in summertime (Sun et al., 2010). Both POAs (Zou et al., 2016) and SOAs (Chowdhury et al., 2018; Gaschen et al., 2010) in the atmosphere exert cytotoxic effects on the human respiratory system. Nordin et al. (2015) concluded that the variation in the abundance of organic compounds, such as polycyclic aromatic hydrocarbons (PAHs), which are emitted from wood combustion, is the main factor influencing toxicological effects. A study on PM_{10} health effects by both acellular and cell line methods demonstrated that the significant ecotoxic and cytotoxic response were depending on the chemical compositions (Lionetto et al., 2019).

Oxidative stress and inflammation are fundamental and critical mechanisms in PM-induced pulmonary diseases (Dieme et al., 2012). In vitro experiments have revealed that an imbalance between pro-oxidants and antioxidants causes inflammatory reactions and even exacerbates existing inflammatory diseases in the human lung (Jia et al., 2017; Terzano et al., 2010). The variety of organic compounds in PM could directly or indirectly contribute to the induction of oxidative and inflammatory reactions in the human respiratory system through metabolic activation (Abbas et al., 2016; Boublil et al., 2013; Dergham et al., 2015). Even exposure to low doses of $PM_{2.5}$ could induce early cell cycle arrest and cause DNA damage because of the high proportion of PAHs (Longhin et al., 2013b). Compared with $PM_{2.5}$, quasi-ultrafine particles (PM_1, diameter < 1 μm) have a higher toxic potential because of their greater concentrations and surface areas (Daher et al., 2014). PM_1 can carry and deliver more redox-active organic compounds to the respiratory system than large particles, leading to a cascade of adverse effects related to oxidative stress and inflammation in the lungs and even in extrapulmonary sites (Delfino et al., 2010b).

Both primary and secondary organic components in PM_1 are crucial determinants of cytotoxicity in studies on pulmonary health effects. A combination of online monitoring and offline OA analysis could provide knowledge on not only the characteristics of individual organic components but also the potential sources of OAs. Mong Kok (MK), an urban district in Hong Kong with dense buildings and traffic, suffered with heavy pollution (Louie et al., 2005). The objectives of this study were as follows: 1) to characterize organic components in PM_1 and investigate major sources in an urban area by using both online and offline approaches and 2) to identify principal organic chemical compounds and organic sources that contributed to the activation of cytotoxicity in the human respiratory system by performing toxicological experiments with human lung alveolar epithelial (A549) cells.

2. Methodology

2.1. Sampling protocol

The measurements of air pollutants were conducted at a roadside air quality monitoring station of the Hong Kong Environmental Protection Department (HKEPD) in MK (Fig. S1). The station is located at the junction of Nathan Road and Lai Chi Kok Road, both known for heavy traffic. In addition to many commercial and residential buildings, a variety of businesses, such as restaurants and small-to-medium–sized stores, surround the site. Continuous nonrefractory submicron aerosol species (e.g., organic fractions, nitrate, sulfate, ammonium, and chloride) were monitored using an online Quadrupole Aerosol Chemical Speciation Monitor (Q-ACSM, Aerodyne Research Billerica, MA, USA) from March 31 to April 20, 2017. PM_1 samples were collected on 47-mm Teflon (Pall Life Sciences, Ann Arbor, MI, USA) and 47-mm quartz fiber filters (Whatman Inc., Clifton, NJ, USA) by using a PM_1 cyclone sampler (URG-2000-30EHB, URG Corporation, NC, USA) from March 16 to April 23, 2017. Air was drawn through a PM_1 inlet at a calibrated flow rate of 16.7 L min^{-1} and then equally divided into two channels for collection of particles onto the Teflon and quartz fiber filter, respectively. Twenty-four-hour integrated PM_1 samples were collected in 2-day intervals during the sampling period. The concentration levels of gaseous species, including carbon monoxide (CO), sulfur dioxide (SO_2), nitrogen monoxide/oxides (NO/NO_x), and ozone (O_3), were reported by various analyzers operated by the HKEPD at the station. Meteorological data (i.e., wind speed, wind direction, relative humidity, temperature, pressure, precipitation, and solar radiation) were achieved from the Hong Kong Observatory, which is located approximately 1.5 km from the sampling station.

2.2. Instrumentation for online measurements

The Q-ACSM is used for real-time and long-term continuous observation of the chemical composition of submicron particles. Details regarding the principles of Q-ACSM are reported by Ng et al. (2011). Briefly, particles with a size ranging from approximately 40 to 1000 nm converge into a very narrow particle beam through the aerodynamic lens in front of the Q-ACSM. After passing through a vacuum chamber, the particle beam reaches the detection chamber where nonrefractory chemical components are instantly vaporized at 600 °C. The chemical components are then ionized by a 70-eV electron impact source. Positively charged ions are then measured and quantified using a quadrupole mass spectrometer.

In this study, a sampling pump that operated at 3 L min^{-1} was used to introduce atmospheric particles through a stainless-steel tube (external diameter of 0.5"). Part of the flow (84 cc min^{-1}) was sampled into the Q-ACSM. The PM_1 Sharp Cut Cyclone (Rupprecht & Patashnick Co, Inc., NY, USA) was installed in front of the outdoor sampling tube to remove coarse particles in the atmosphere. The Q-ACSM was equipped with a Nafion dryer (MD-110-48S; Perma Pure, Inc., Lakewood, NJ, USA) to remove moisture in the air stream because moisture can reduce detections.

The calibration of the ionization efficiency (IE) of the Q-ACSM was performed as follows. NH_4NO_3 was atomized, dried, and then screened with a particle size of 300 nm by using a differential mobility analyzer (DMA, Model 3080, TSI, MN, USA). Selected NH_4NO_3 particles were sampled into the Q-ACSM and condensation particle counter (CPC, Model 3772, TSI, MN, USA). The IE was determined by comparing the responses of ions for nitrate (i.e., *m/z* 30 and 46) of the 300-nm particle measured using the Q-ACSM with their mass concentration and particle numbers measured using DMA and CPC, respectively. The response factor that converted the signal into mass concentration could then be obtained. The standard relative IEs for sulfate and ammonium from the IE calibration were 0.89 and 4.81, respectively.

2.3. Offline analysis

Teflon filters were used for the gravimetric measurement by using a microbalance (Model MC5, Sartorius, Göttingen, Germany) with a precision of approximately 1 μg. Filter preparation and gravimetric analysis were conducted in a high-efficiency particulate absorption (HEPA) clean room in compliance with ISO 14644 (Class 7) at The Hong Kong Polytechnic University. The initial and final mass determinations were conducted within 30 days before sampling. Post-sampling weighing procedures were performed within 30 days before and after the sampling period. All particle-loaded filters were stored at −20 °C for further chemical and toxicological analyses.

Organic speciation was conducted using quartz fiber filter samples. The filters were pre-heated at 900 °C for 3 h to remove any organic contaminants before sampling. Nonpolar organics, including n-alkanes, iso-/antiiso-alkanes, hopanes, steranes, PAHs, and oxy-PAHs (OPAHs) were quantified using in-injection port thermal desorption−gas chromatography/mass spectrometry (TD-GC/MS). Polar monocarboxylic acids were analyzed through solvent extraction (SE)-GC/MS method. The target organic species and their abbreviations are listed in Table 1. Portions of 1 cm^2 and 5 cm^2 of the quartz filter sample were used for TD and SE-GC/MS analyses, respectively. For SE, extraction recoveries for monocarboxylic acids ranged from 82% to 98%. The details of sample preparation, extraction, calibration, and instrumental settings were described by Ho and Yu (2004), Feng et al. (2006), and Ho et al. (2011).

2.4. Cell experiments

A549 cells obtained from the American Type Culture Collection (ATCC, Manassas, VA, USA) were cultured in Roswell Park Memorial Institute medium (10% fetal bovine serum, penicillin, and streptomycin) in a humidified 95% air and 5% CO_2 incubator at 37 °C. The cells (at a density of 10^5 cells/mL) were exposed to 0 μg/mL (control) and 50 μg/mL of PM_1 extractions for 24 h. Each experiment was conducted in triplicate, at least.

Reactive oxygen species (ROS) production was determined using the fluorogenic cell-based method by using 2′,7′-dichlorodihydrofluorescein diacetate (DCFH-DA) as a probe. The oxidative reaction of DCFH-DA with ROS produces a highly fluorescent compound of 2′,7′-dichlorofluorescin, enabling the detection of the dominant cellular ROS by the probe. After the cells were exposed to DCFH-DA, the fluorescence intensity was determined using a Light Luminescence Plate Reader (VICTOR X; PerkinElmer, Waltham, MA, USA) at excitation and emission wavelengths of 485 and 530 nm, respectively. The cellular oxidative stress was presented as the fluorescence intensity (FI).

Lactic dehydrogenase (LDH) and interlukin-6 (IL-6) in cell supernatants, as indicators of cytotoxicity and inflammation levels, were measured using enzyme-linked immunosorbent assay (ELISA) kits (BD Biosciences, CA, USA) according to manufacturer's instructions.

2.5. Data analysis

2.5.1. ACSM data processing

Igor-based Q-ACSM data processing software (Aerodyne Research) was used to obtain nonrefractory-PM_1 (NR-PM_1) chemical components. The collection efficiency (CE) of each chemical component was corrected according to the following equation: CE_{dry} = max (0.45, 0.0833 + 0.9167 × ANMF), as described by Middlebrook et al. (2012).

2.6. Source apportionment

Positive matrix factorization (Paatero, 1997; Paatero and Tapper, 1994) is typically used to resolve organic sources. It is a bilinear model representing data entered as a linear combination of the factor's time series and static profiles as follows:

$$X = GF + E \tag{1}$$

where X is the measured matrix consisting of *j* columns and *i* rows, G is the factor's time series, F is the corresponding profile, and E is the residuals of the model. The iterative minimization of Q (defined in equation (2)) was conducted using a least squares approach.

$$Q = \sum_{i=1}^{m}\sum_{j=1}^{n}\left(\frac{e_{ij}}{\sigma_{ij}}\right)^2 \tag{2}$$

where e_{ij} is the squared residual and σ_{ij} is the uncertainty. According to equation (2), Q is defined as the sum of e_{ij} weighted by their respective σ_{ij}.

Three factors were resolved using via PMF runs, namely POA, less-oxidized oxygenated OA (LO-OOA), and more-oxidized oxygenated OA (MO-OOA) (Fig. S2). The mass spectrum of POA is prominent in hydrocarbon ions, including $[C_nH_{2n+1}]^+$ and $[C_nH_{2n-1}]^+$. The mass spectra of LO-OOA and MO-OOA are characterized by high signals at *m/z* 44, which is the marker for secondary organics (Fig. S2). MO-OOA had higher signals at *m/z* 44 than did LO-OOA, suggesting a higher oxygenation level in MO-OOA.

Table 1
Abbreviations for all target individual organic compounds quantified in this study.

Organic Compounds	Abbreviation	Organic Compounds	Abbreviation	Organic Compounds	Abbreviation	Organic Compounds	Abbreviation
Alkanes		**Hopanes**		**PAHs**		**Organic acids**	
Pentadecane	n-C_{15}	22,29,30-trisnorneophopane	Ts	Acenaphthylene	ACY	Hexanoic acid	C_6
Hexadecane	n-C_{16}	22,29,30-trisnorphopane	Tm	Acenapthene	AC	Heptanoic acid	C_7
Heptadecane	n-C_{17}	αβ-norhopane	C29αβ	Fluorene	FLO	Octanoic acid	C_8
Octadecan	n-C_{18}	βα-norhopane	C29βα	Phenanthrene	PHE	Nonanoic acid	C_9
Nonadecane	n-C_{19}	αβ-hopane	C30αβ	Anthracene	ANT	Decanoic acid	C_{10}
Icosane	n-C_{20}	βα-hopane	C30βα	Fluoranthene	FLT	Undecanoic acid	C_{11}
Heneicosane	n-C_{21}	αβS-homohopane	C31αβS	Pyrene	PYR	Dodecanoic acid	C_{12}
Docosane	n-C_{22}	αβR-homohopane	C31αβR	Benzo [a]anthracene	BaA	Tridecanoic acid	C_{13}
Tricosane	n-C_{23}	αβS-bishomohopane	C32αβS	Chrysene	CHR	Tetradecanoic acid	C_{14}
Tetracosane	n-C_{24}	αβR-bishomohopane	C32αβR	Benzo [b]fluoranthene	BbF	Pentadecanoic acid	C_{15}
Pentacosane	n-C_{25}	22S-trishomohopane	C33αβS	Benzo [k]fluoranthene	BkF	Hexadecanoic acid	C_{16}
Hexacosane	n-C_{26}	22R-trishomohopane	C33αβR	Benzo [a]fluoranthene	BaF	Heptadecanoic acid	C_{17}
octacosane	n-C_{27}	22S-tretrahomohopane	C34αβS	Benzo [e]pyrene	BeP	Octadecanoic acid	C_{18}
nonacosane	n-C_{28}	22R-tetrashomohopane	C34αβR	Benzo [a]pyrene	BaP	Nonadecanoic acid	C_{19}
Nonacosane	n-C_{29}	22S-pentashomohopane	C35αβS	Perylene	PER	Eicosanoic acid	C_{20}
Triacontane	n-C_{30}	22R-pentashomohopane	C35αβR	Indeno [1,2,3-cd]pyrene	IcdP	Heneicosanoic acid	C_{21}
Hentriacotane	n-C_{31}	**Steranes**		Dibenzo [a,h]anthracene	DahA	Docosanoic acid	C_{22}
Dotriacontane	n-C_{32}	ααα 20R-Cholestane	ααα-20R−C	Benzo [ghi]perylene	BghiP	Tricosanoic acid	C_{23}
Tritriactotane	n-C_{33}	ααα 20S-Cholestane	ααα-20S−C	Coronene	COR	Tetracosanoic acid	C_{24}
Tetratriactoane	n-C_{34}	αββ 20R-Cholestane	αββ-20R−C	**OPAHs**		Pentacosanoic acid	C_{25}
Pentatriacontane	n-C_{35}	αββ 20S-Cholestane	αββ-20S−C	9-Fluorenone	9-FLU	Hexcosanoic acid	C_{26}
Hexatriacontane	n-C_{36}	βαα 20R-Cholestane	βαα 20R−C	1,8-Napthalic anhydride	1,8-NAP	Heptacosanoic acid	C_{27}
Heptatriacotane	n-C_{37}	ααα 20S 24S-Methylcholestane	ααα-20S−24S-MEC	Anthroquinone	ANQ	Octacosanoic acid	C_{28}
Ocatriacotane	n-C_{38}	αββ 20R 24S-Methylcholestane	αββ-20R-24S-MEC	Methylfluoranthene	MEFLO	Nonacosanoic acid	C_{29}
Iso-/Antiiso-Alkanes		αββ 20S 24S-Methylcholestane	αββ-20S−24S-MEC	Cyclopenta [cd]pyrene	CcdPYR	Triacontanoic acid	C_{30}
Iso-nonacosane	iso-C_{29}	ααα 20R 24R-Methylcholestane	ααα-20R-24R-MEC	Retene	RET	Hentriacontanoic acid	C_{31}
Anteiso-nonacosane	anteiso-C_{29}	ααα 24R-Ethylcholestane	ααα-24R-EC	Methylchrysene	MECHR	Dotriacontanoic acid	C_{32}
Iso-triacontane	iso-C_{30}	ααα 20S 24R/S-Ethylcholestane	ααα-20S-24R/S-EC	Benz [a]anthracene-7,12-dione	BANTdione	Tritriactotanoic acid	C_{33}
Anteiso-triacontane	anteiso-C_{30}	ααα 20S 24R/S-Ethylcholestane	ααα-20S-24R/S-EC	Dibenzo [a,e]pyrene	DaePYR	Tetratriactoanoic acid	C_{34}
Iso-hentriacotane	iso-C_{31}	αββ 20S 24R-Ethylcholestane	αββ-20S-24R-EC			pinonic acid	PIN
Anteiso-hentriacotane	anteiso-C_{31}	ααα 20R 24R-Ethylcholestane	ααα-20R-24R-EC			palmitoleic acid	C16:1
Iso- dotriacontane	iso-C_{32}	βαα 20R 24R-Ethylcholestane	βαα-20R-24R-EC			oleic acid	C18:1
Anteiso-dotriacontane	anteiso-C_{32}	4α-Methyl-24R-ethyl-5α(H),14α(H),17α(H)-cholestane	4α-M-24R-E-C			linoleic acid	C18:2
Iso-tritriactotane	iso-C_{33}	4α-Methyl-5α(H),14α(H),17α(H)-cholestane	4α-M-C			linolenic acid	LIN
Anteiso-tritriactotane	anteiso-C_{33}					pimaric acid	PIM
						abietic acid	ABI

2.6.1. Correlation analysis

One-way analysis of variance (ANOVA) was used to examine the statistical significance of between-group differences. Pearson's correlation coefficient and a stepwise regression model were used to assess correlations between bioactivity markers, LDH, ROS, and IL-6 and organic compounds. Statistical analyses were performed using SPSS version 12.0 (SPSS Inc., Chicago, IL, USA). The level of significance was set at $p < 0.05$.

3. Results and discussion

3.1. Concentrations and chemical composition

The NR-PM_1 (non-refractory components in PM with an aerodynamic diameter less than 1 μm) concentration ranged from 3.2 to 68.2 μg m^{-3}, with an average of 25.1 ± 12.1 μg m^{-3}. NR-PM_1 contributed to 84% of the PM_1 concentrations. NR-PM_1 was more correlated with the sum of secondary components (i.e., sulfate,

nitrate, ammonium, LO-OOA, and MO-OOA) than with primary components (i.e., POA and chloride), suggesting that the variation in NR-PM_1 was mainly driven by secondary processing (Fig. S3).

Fig. 1 illustrates the chemical composition of NR-PM_1. Organics contributed most to the NR-PM_1 concentration, with a mass fraction of 55% ± 15% (14 ± 8.2 μg m^{-3}), followed by sulfate (21% ± 8.9%, 5.3 ± 2.7 μg m^{-3}), ammonium (13% ± 6.0%, 3.3 ± 1.8 μg m^{-3}), nitrate (10% ± 6.0%, 2.5 ± 2.4 μg m^{-3}), and chloride (1.0% ± 1.0%, 0.3 ± 0.2 μg m^{-3}). Chemical compositions observed in this study are consistent with those reported in previous studies in Hong Kong. Sun et al. (2016) found that the mass fraction of organics in NR-PM_1 was the major component in Kowloon peninsula, which includes MK district. By contrast, sulfate was found to be the largest component in other suburban areas (Li et al., 2013, 2015). Differences in chemical compositions between downtown and suburban areas in Hong Kong can be explained as follows. First, the downtown area is often influenced by local sources, such as traffic and cooking emissions (Sun et al., 2016), that release primary organics and the precursors of secondary organics. However, suburban areas are mainly affected by regional sources (Li et al., 2013, 2015). Because other components, such as organics, nitrate, ammonium, and chloride, can be depleted more efficiently than sulfate during long-range transport, sulfate is the largest component contributed by regional transport (Lanz et al., 2010).

Fig. 2 presents the diurnal variations of chemical components in NR-PM_1. The organics peaked at 08:00, 13:00, and 19:00–20:00, corresponding to increases in traffic and cooking emissions during rush hours and mealtimes. Similar observations were also reported in the downtown area of Hong Kong during autumn and winter (Sun et al., 2016), suggesting the phenomenon was less affected by seasonal factors. The abundance of sulfate increased gradually from 11:00 to 17:00, indicating that its formation strength outweighed the dilution effect of the increase in planetary boundary layer height. Nitrate gradually decreased from 05:00 to 10:00 but exhibited a valley in the afternoon, consistent with the increase in ambient temperature in the early daytime; nitrate decreased because evaporation together with the vertical dilution caused by the mixing layer dynamics (Dinoi et al., 2017) outweighs formation. The diurnal pattern of ammonium was similar to that of sulfate, suggesting their close relation in the urban atmosphere. The chloride concentration was likely governed by accumulation and temperature-induced evaporation, maintaining a high level during the day, declining in the early morning, and then exhibiting a valley in the midafternoon.

3.2. Sources of organic aerosols

Three organic sources were resolved, namely POA, LO-OOA, and MO-OOA. The time series of POA was highly correlated with the markers *m/z* 55 ($C_4H_7^+$), 57 ($C_4H_9^+$), and 69 ($C_5H_9^+$) (R^2 = 0.86–0.90). The time series of the secondary organics LO-OOA and MO-OOA were correlated with *m/z* 43 (R^2 = 0.60 for LO-OOA and R^2 = 0.15 for MO-OOA) and *m/z* 44 (R^2 = 0.20 for LO-OOA and R^2 = 0.82 for MO-OOA). Subsequently, the time series of the three organic sources were compared with gas and chemical species (Table S1). The results further indicated that POAs were more correlated with primary tracers (i.e., NO_x and CO), whereas OOAs were more correlated with secondary tracers (i.e., O_3, sulfate, nitrate, and ammonium).

Fig. 3 illustrates the mass compositions of organic sources. POA contributed 40% ± 19% (5.5 ± 4.2 μg m^{-3}) of the total organic mass concentration, followed by MO-OOA (32% ± 22%, 4.4 ± 3.4 μg m^{-3}) and LO-OOA (28% ± 19%, 3.9 ± 3.3 μg m^{-3}). The compositions were similar to those reported for Hong Kong's urban area (Sun et al., 2016) where POA contributed 42% of the organic mass. The mass compositions of POA were higher in the downtown area than in suburban areas; Li et al. (2013, 2015) reported this difference to be between 20% and 30%. POA is often dominated by local sources, and OOA is mainly influenced by regional contributions (Ng et al., 2011).

Fig. 2 reveals diurnal variations in organic sources. The POA trend exhibited two prominent peaks at lunch (13:00) and (19:00–20:00) dinner times. The contribution of POA to total organics was 45%–52% during the two periods. POA did not show peak at 8:00 of the rush hour, which is likely due to the fact that most shops open after 9:00 a.m., causing the primary emissions to continue to rise after the morning rush hours. The diurnal trend of LO-OOA also revealed peaks during rush hours and mealtimes, which is likely due to the rapid oxidation of primary organics and the production of secondary species. The composition of MO-OOA remained relatively stable throughout the day, indicating that it was likely contributed from regional transport.

3.3. Organic speciation

Temporal variations in total quantified n-and iso-/antiiso-alkanes, hopanes, steranes, PAHs, OPAHs, and organic acids are listed in Fig. 4. The molecular distributions of these organic classes are presented in Figs. S4–S7. The total quantified concentration of *n*-alkanes (n-C_{15} to n-C_{38}) ranged from 162.7 to 556.2 ng m^{-3}, with an average value of 325.0 ± 97.4 ng m^{-3}. POA was significantly

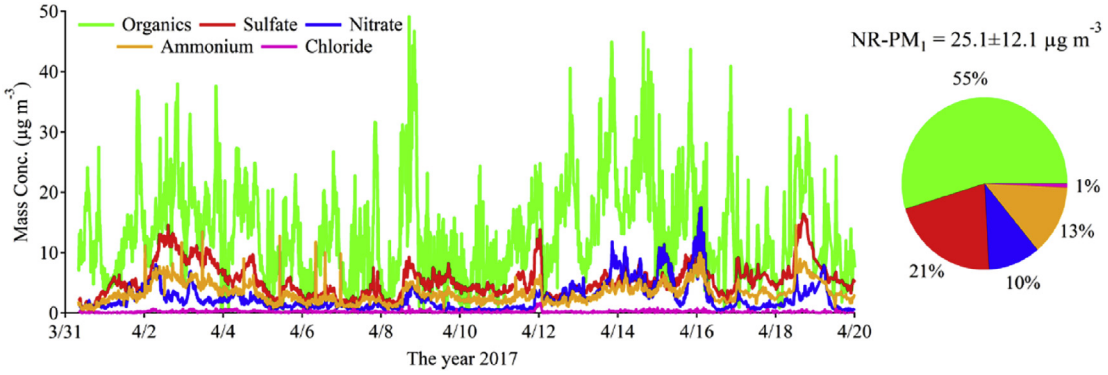

Fig. 1. Time series of NR-PM_1 chemical components and their compositions (shown in pie-chart).

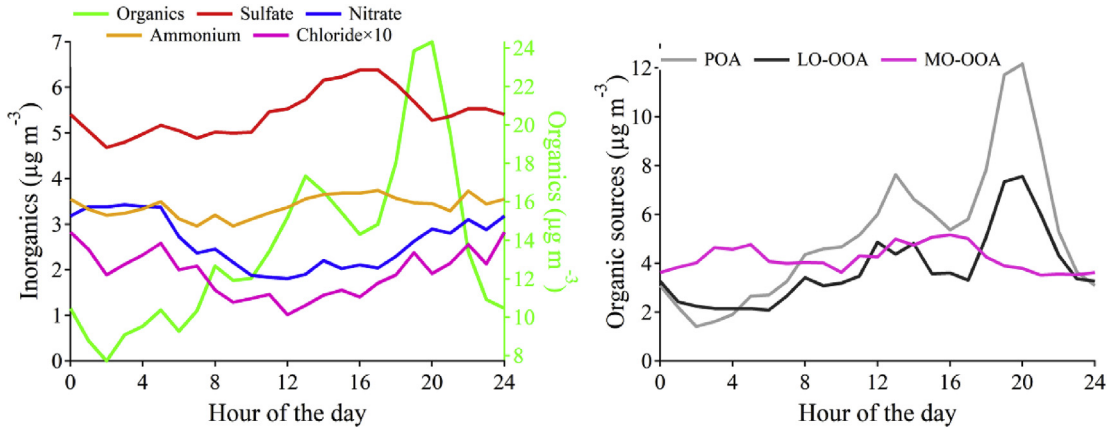

Fig. 2. Diurnal variations of NR-PM_1 chemical components and organic sources.

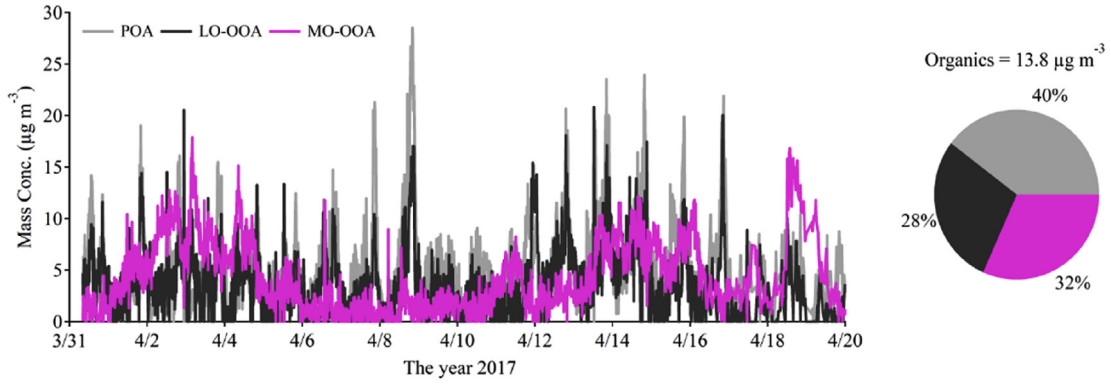

Fig. 3. Time series of organic sources and their compositions (shown in pie-chart).

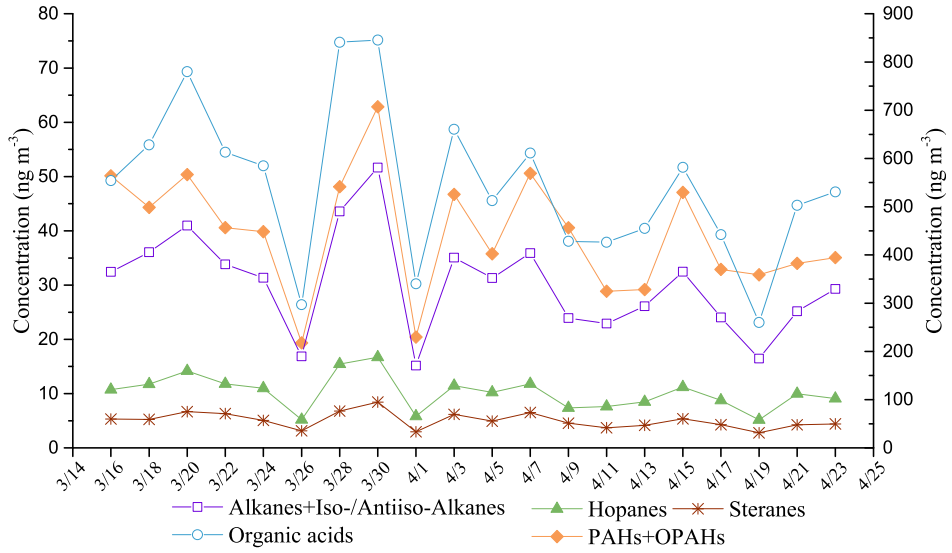

Fig. 4. Variations of five organic classes in PM_1 during the sampling period (right vertical axis was for alkanes and organic acids and the left vertical axis was for other three chemical classes).

correlated ($p < 0.05$) with n-C_{18} ($R = 0.67$), iso-C_{31} ($R = 0.68$), and anteiso-C_{32} ($R = 0.69$). C_{27}, C_{29} and C_{31}, which are always distinguished as the markers of fossil fuels sources (Simoneit et al., 1988), has been showed higher concentrations among the individual alkanes. The carbon maximum number (C_{max}; the *n*-alkane exhibiting the highest concentration among homologs) and the carbon preference index (CPI; the concentration ratio of odd-to even numbered homologs) are widely used as indicators for the

contributions of anthropogenic and biogenic sources (Simoneit et al., 1988). The C_{max} was at C_{31} (44.8 ± 15.8 ng m^{-3}), and the average CPI was 1.4 (ranging from 1.0 to 1.7). These values suggested that *n*-alkanes at this roadside site were codominated by fossil fuel combustion (i.e., gasoline- and diesel-fueled vehicle emissions) and cooking emissions.

Hopanes are tracers for fossil fuel residue, particularly from vehicular emissions, because of their stability in the atmosphere (He et al., 2006). The total quantified hopane concentration was 10.2 ± 3.1 ng m^{-3} on average, ranging from 5.17 to 16.7 ng m^{-3}. The most abundant hopane was C30αβ (2.0 ± 0.6 ng m^{-3}), followed by C29αβ (1.8 ± 0.6 ng m^{-3}) and C31αβS (1.3 ± 0.4 ng m^{-3}). Ts (R = 0.68), C29βα (R = 0.70), C30βα (R = 0.90), and C31αβR (R = 0.68) were significantly correlated with POA ($p < 0.05$). The concentration and distribution of hopanes observed in this study are consistent with those reported at an urban site in Shanghai revealing the influence of engine exhausts (Feng et al., 2012). Significant correlations between hopanes and alkanes (R^2 = 0.98, Fig. S8) also suggested that vehicle emissions are the dominant source of both alkanes and hopanes. Steranes, which are constituents of lubricating oils, are also indicators of traffic emission (Mikuška et al., 2015). The average total quantified steranes was 5.1 ± 1.4 ng m^{-3}. The most abundant individual sterane in MK was αββ-20R–C, followed by βαα 20R–C, αββ-20R-24S-MEC, and ααα-20S-24R/S-EC.

The average total quantified concentration of PAHs and OPAHs was 39.4 ± 10.6 ng m^{-3}, with a range of 19.4–62.9 ng m^{-3}. Fluoranthene (FLT; 3.3 ± 1.1 ng m^{-3}) was the most abundant individual PAH, followed by benzo [ghi]perylene (BghiP; 2.6 ± 0.8 ng m^{-3}) and benzo [b]fluoranthene (BbF; 2.5 ± 0.9 ng m^{-3}). The most abundant OPAH was 1,8-napthalic anhydride (1,8-NAP; 11.6 ± 3.8 ng m^{-3}). The relative abundance of alkyl-PAHs indicated that chiefly derived from traffic sources, especially diesel vehicles (Barakat, 2002). Both BghiP, which has been recognized as a tracer for vehicular emission (Gao et al., 2013), and the diagnostic ratio of BghiP to benzo [e] pyrene (BeP; 1.26 on average, ranging from 0.92 to 1.58) indicated the major contribution of vehicle exhaust at the MK station (Nielsen, 1996). The diagnostic ratio of indeno [1,2,3-cd]pyrene (IcdP) to the sum of IcdP and BghiP has also been used for differentiating vehicular emissions (<0.4) from coal, wood, and grass combustion (>0.5) (Xu et al., 2016). The average IcdP/(IcdP + BghiP) ratio was 0.42 (ranging from 0.35 to 0.47), suggesting that PAHs mainly originated from vehicle emission, whereas the contributions of coal combustion and biomass burning were negligible. In addition, PAHs were highly correlated with hopanes (R^2 = 0.74, Fig. S8), demonstrating that fossil fuel combustion, particularly that of vehicle exhausts, was the dominant source of these classes of organics.

The average concentration of total quantified fatty acids was 544.7 ± 158.0 ng m^{-3}, ranging from 59.90 to 845.4 ng m^{-3}. Among individual fatty acids (C_6–C_{34}), C_{16} and C_{18} were the two most abundant species, with average concentrations of 160.9 ± 49.1 and 77.7 ± 23.3 ng m^{-3}, respectively. Moreover, POA correlated well with C_{11} (R = 0.797, $p < 0.01$) and C_{21} (R = 0.658, $p < 0.05$). The distribution of fatty acids was similar to that in urban Beijing (Huang et al., 2006). Homologs < C_{20} are ubiquitous and are produced from anthropogenic sources such as cooking and fossil fuel combustion (Rogge et al., 1991), whereas homologs > C_{22} originate from vascular plant wax (Simoneit and Mazurek, 1982). Profiles suggested the strong and extensive contribution of cooking emission to fatty acids in MK. The great abundance of alkanoic acids served as additional strong evidence (Rogge et al., 1991). Three alkanoic acids, namely palmitoleic ($C_{16:1}$), oleic ($C_{18:1}$), and linoleic ($C_{18:2}$) acid, were detected, and their concentration levels were relatively high, particularly for $C_{18:1}$ (62.4 ± 19.4 ng m^{-3}) and $C_{18:2}$ (11.5 ± 5.0 ng m^{-3}). Our results are consistent with the high composition of alkanoic acids observed in samples collected in a dense commercial restaurant area in China (Feng et al., 2006).

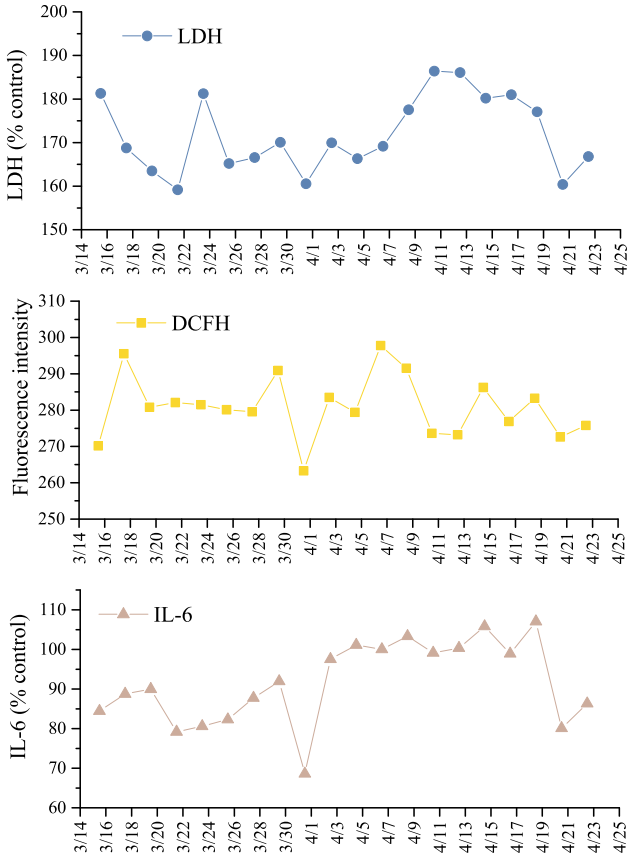

Fig. 5. Sequential bioreactivity caused by PM_1 at a dose of 50 μg/ml in A549 cells, including a) lactate dehydrogenase (LDH, % control), b) DCFH presented by fluorescence intensity and c) interleukin-6 (IL-6, % control).

3.4. PM_1 cytotoxicity

Cytotoxicity induced by PM_1 collected at the MK site is illustrated in Fig. 5. Compared with experimental controls, LDH and IL-6 levels in A549 cells significantly increased after exposure to PM_1, indicating cytotoxic and inflammatory reactions, respectively. Furthermore, DCFH, which indicated that ROS generation triggered by PM_1, also revealed increased levels after exposure. Similar results were also reported by Bekki et al. (2016).

Because of variations in the chemical composition, the intensity of cytotoxicity varied among sampling days. For example, LDH and IL-6 levels on April 11 and 13 were higher than those on other dates. A high contribution of organics was observed for the corresponding period, ranging from 55.6% to 61.7% of PM_1 mass. The crucial role of organic compounds in triggering oxidative and inflammation response in A549 cells has been confirmed in previous studies (Ho et al., 2016; Sun et al., 2018; Wu et al., 2017). Obvious variations in cytotoxicity in A549 cells demonstrated oxidative and inflammatory reactions induced by organic components. Extractable organic compounds in PM, such as PAHs, are associated with early oxidative reactions that are supported by the NRF-2 signaling pathway (Abbas et al., 2019). Polar organics in $PM_{2.5}$ could irritate the secretion of cytokines, including IL-6 in BEAS-2B, which modulate the inflammatory response in the lung (Fuentes-Mattei et al., 2010).

Organic components in PM_1 might activate the aryl hydrocarbon

receptor (AhR) in A549 cells, resulting in increased expression in AhR-regulated genes, which subsequently induces various toxic effects on targeted cells (Longhin et al., 2013a). An increase in LDH in cells was referred to earlier alterations in mitochondrial metabolism and cell proliferation but later induces disruption of membrane integrity and/or permeability (Dergham et al., 2012). Variations in oxidative stress and inflammation are crucial mechanisms underlying PM-induced respiratory effects, which include decreased pulmonary function and mediation of the development, maintenance, and exacerbation of airway obstructive diseases (Feng et al., 2016). Excessive production of ROS that exceeds the detoxification capacity of antioxidant scavengers and enzymes results in changes in the redox status of A549 cells (Dieme et al., 2012). Adverse effects on cells triggered by excess ROS through reactions with biomacromolecules (i.e., plasmatic lipids, proteins, and DNA) include impairing their structures and functions and ultimately increasing damage to target cells and tissues (Jomova and Valko, 2011). Subsequently, a cascade of effects associated with inflammation could be triggered after inducing oxidative stress in A549 cells, which significantly contribute to the development and exacerbation of respiratory diseases (Lonkar and Dedon, 2011).

3.5. Correlations between organics and bioactivities

Correlations between cytotoxicity and organic sources and organic compounds in PM_1 are presented in Table 2. For the three identified organic sources, only POA was significantly associated with DCFH ($R = 0.69$, $p < 0.05$) and IL-6 ($R = 0.86$, $p < 0.01$). OAs from primary emissions were more correlated with oxidative stress and inflammatory reactions triggered in the human respiratory system. However, oxidized OAs did not exhibit significant correlations with cytotoxicity. The five organic classes revealed medium ($0.3 < R < 0.7$) to high ($R \geq 0.7$) correlations ($p < 0.01$) with LDH, indicating that they were significant contributors to cytotoxicity in A549 cells. DCFH was correlated with alkanes and iso/antiiso-alkanes ($R = 0.47$, $p < 0.05$), steranes ($R = 0.51$, $p < 0.05$), and PAHs and OPAHs ($R = 0.57$, $p < 0.01$). IL-6 was highly correlated ($p < 0.01$) with all five classes of organic compounds, indicating their potential contribution to inflammation. Chuang et al. (2018) demonstrated that emissions from major industries were associated with increases in oxidative stress and inflammation; the authors concluded that petrochemical-emitted $PM_{2.5}$ threatened the health of surrounding residents, which is consistent with the current study's results. A study on the generation of ROS concluded that motor vehicle emissions and coal combustion sources were more important contributors to ROS in $PM_{2.5}$ than other sources (Wang et al., 2020).

Table 2
Correlations between the cytotoxicity [lactate dehydrogenase (LDH), DCFH and interleukin-6 (IL-6)] and organic sources and organic compounds in PM_1.

	LDH	DCFH	IL-6
Organic sources			
POA	0.575	**0.688***	**0.862****
LO-OOA	−0.243	0.142	−0.208
MO-OOA	0.094	−0.404	0.038
Organic compounds			
Alkanes + Iso-/Antiiso-Alkanes	**0.675****	**0.472***	**0.945****
Hopanes	**0.677****	0.386	**0.957****
Steranes	**0.721****	**0.505***	**0.909****
PAHs + OPAHs	**0.653****	**0.576****	**0.862****
Organic acids	**0.668****	0.370	**0.968****

*p<0.05, **p < 0.01.

Correlations between individual organic compounds and bioreactivity are presented in Table S2. Most compounds exhibited medium to high correlations ($p < 0.05$) with bioreactivity, particularly with LDH and IL-6. Chemical compositions play crucial roles in stimulating the generation of oxidative and inflammatory cytokines (Velali et al., 2016; Xu et al., 2018), and organic compounds might have distinct capacities to generate superoxide and hydroxyl radicals and finally induce extensive oxidative and inflammatory reactions (Chuang et al., 2019). Alkanes, such as n-$C_{25,29,35}$, were highly correlated ($R > 0.90$) with IL-6, but only a few of n-$C_{22,28,33,35}$ were significantly correlated with ROS generation. For hopanes and steranes, C33αβS, C35αβR, and βαα 20R−C revealed high correlations with both LDH ($R > 0.65$) and IL-6 ($R > 0.70$). Notably, most of the individual PAHs and OPAHs correlated well with LDH ($R > 0.5$), IL-6 ($R > 0.6$), and ROS generation ($R > 0.4$). Organic acids were highly correlated with IL-6 ($R > 0.7$), demonstrating their contribution to inflammatory reactions. Naimabadi et al. (2016) highlighted the contribution of organic compounds in PM to cytotoxicity. Oh et al. (2011) reported that organic compounds in PM extracts are important causative agents. Organic compounds, such as PAHs, can induce toxic effects through the formation of ROS and the induction of inflammatory responses during their biotransformation by cytochrome P-450 1A1 (Alkurdi et al., 2014; Delfino et al., 2010a). A study investigated the oxidative potential of aerosols find that toxic substances related to ROS generation are generally substances with conjugated electrons, such as PAHs and O-PAHS (Chen et al., 2019). The variation in oxidative and inflammatory reactions could be caused by different pathways or mechanisms related to the composition of organic compounds (Happo et al., 2013). For example, PAHs induce cytotoxicity through pathways involving the expression of nuclear transcription factor-κB, which can increase the transcription of cytokines and acute-phase proteins (Riedl and Diaz-Sanchez, 2005).

Primary organic components in PM_1 at the MK site were significantly correlated with cytotoxicity, indicating the dominant role of primary emissions in A549-cell cytotoxicity. The environmentally persistent free radical (EPFR) in PM which were carbon-centered with a nearby heteroatom also contributed to the generation of ROS as POA (Chen et al., 2018). A chamber study found that dark-aged PM reduced viability and generation of inflammatory markers in comparison with fresh PM. The variation in toxicity could be caused by secondary particles that formed from PAHs and other organic compounds (Nordin et al., 2015). Hopanes, including Tm, C29αβ, and C30αβ, and PAHs, including BaP, PER, IcdP, and BghiP, have been identified as petroleum-related organic tracers in the atmosphere (Wang et al., 2016; Yang et al., 2005). These compounds exhibited medium to high correlations with LDH and IL-6, and perylene (PER) and BghiP were significantly correlated with ROS generation. All of these correlations emphasize the contribution of vehicular emission to human respiratory effects. Furthermore, our results are consistent with the finding that exposure to diesel exhaust $PM_{2.5}$ collected in an urban area could activate IL-6 transcription (Baulig et al., 2003). Künzi et al. (2013) further concluded that diesel exhaust PM had stronger effects on cells than did wood combustion PM. The homologs $< C_{20}$ of fatty acids, which are derived from meat cooking and fossil fuel combustion (He et al., 2006), were relatively highly correlated with LDH and IL-6. Because of the abundance of restaurants in MK, cooking is a major primary emission source in the area. This explains cooking emissions contributed to toxicity in A549 cells. Liu et al. (2015) suggested that $PM_{2.5}$ derived from cooking oil fumes could eventually result in apoptosis mediated by increases in oxidative stress and accompanied by endoplasmic reticulum stress. These lipid-soluble components in PM_1, including fatty acids and PAHs, may become bioavailable after deposition in the human lungs, and then,

unmetabolized chemical compounds further transform into systemic targets (Gerde et al., 2001).

A stepwise regression model was applied to identify organic species that contributed to cytotoxicity, and results are presented in Table S3. Hopanes (C31αβR, C32αβS, and ααα-20R-24R-EC), PAHs (PHE, FLT, and RET), and fatty acids (C14, C22, C30, LIN, PIM, and ABI) were significant factors ($p < 0.01$) in cytotoxicity induced by PM_1 in MK.

4. Conclusions

This study integrated the source apportionment of OAs and organic compositions with environmental cytotoxicity to investigate bioreactivity induced by PM_1. POA (40%), MO-OOA (32%), and LO-OOA (28%) were identified as the three main sources of OAs. Variations in individual alkanes, iso-/antiiso-alkanes, hopanes, steranes, PAHs, OPAHs, and fatty acids were identified using a filter-based analysis, indicating that vehicular and cooking emission were dominant PM_1 sources. POA correlated well with the generation of LDH and IL-6, indicating the critical role of primary emissions in pulmonary diseases. Organic compounds, including alkanes and iso-/antiiso-alkanes, hopanes, steranes, PAHs and OPAHs, and organic acids exhibited medium to high correlations with cytotoxicity. The organic aerosol composition and sources of PM_1 in MK interacted in a complex manner to cause adverse pulmonary effects. This study demonstrated the importance of POA from traffic and cooking emissions in an urban area of Hong Kong in PM-induced oxidative and inflammatory responses. Further research on airway pathology mechanisms is urgently required.

Credit author Statement

Xinyi Niu: Writing - original draft, Methodology, Yichen Wang: Writing - original draft, Visualization, Steven Sai Hang Ho: Validation, Writing - review & editing, Hsiao-Chi Chuang: Conceptualization, Validation, Resources, Jian Sun: Data curation, Investigation, Linli Qu: Formal analysis, Gehui Wang: Resources, Kin Fai Ho: Conceptualization, Supervision

Declaration of competing interest

The authors declare that they have no known competing financial interests or personal relationships that could have appeared to influence the work reported in this paper.

Acknowledgements

This study was supported by National Natural Science Foundation of China (91644102) and Research Grants Council of the Hong Kong Special Administrative Region of China (Project No. 14212116). We gratefully acknowledge the assistance of Hong Kong Environmental Protection Department (HK EPD) providing the Aerosol Chemical Speciation Monitor to this study.

Appendix A. Supplementary data

Supplementary data to this article can be found online at https://doi.org/10.1016/j.chemosphere.2020.128239.

References

Abbas, I., Badran, G., Verdin, A., Ledoux, F., Roumie, M., Guidice, J.-M.L., Courcot, D., Garçon, G., 2019. In vitro evaluation of organic extractable matter from ambient PM2. 5 using human bronchial epithelial BEAS-2B cells: cytotoxicity, oxidative stress, pro-inflammatory response, genotoxicity, and cell cycle deregulation. Environ. Res. 171, 510–522.

Abbas, I., Verdin, A., Escande, F., Saint-Georges, F., Cazier, F., Mulliez, P., Courcot, D., Shirali, P., Gosset, P., Garçon, G., 2016. In vitro short-term exposure to air pollution PM2. 5-0.3 induced cell cycle alterations and genetic instability in a human lung cell coculture model. Environ. Res. 147, 146–158.

Alkurdi, F., Karabet, F., Dimashki, M., 2014. Characterization and concentrations of polycyclic aromatic hydrocarbons in emissions from different heating systems in Damascus, Syria. Environ. Sci. Pollut. Control Ser. 21, 5747–5759.

Baulig, A., Sourdeval, M., Meyer, M., Marano, F., Baeza-Squiban, A., 2003. Biological effects of atmospheric particles on human bronchial epithelial cells. Comparison with diesel exhaust particles. Toxicol. Vitro 17, 567–573.

Barakat, A.O., 2002. PAHs and petroleum markers in the atmospheric environment of Alexandria city, Egypt. Water, Air, Soil Pollut. 139, 289–310.

Bekki, K., Ito, T., Yoshida, Y., He, C., Arashidani, K., He, M., Sun, G., Zeng, Y., Sone, H., Kunugita, N., 2016. PM2. 5 collected in China causes inflammatory and oxidative stress responses in macrophages through the multiple pathways. Environ. Toxicol. Pharmacol. 45, 362–369.

Boublil, L., Assémat, E., Borot, M.-C., Boland, S., Martinon, L., Sciare, J., Baeza-Squiban, A., 2013. Development of a repeated exposure protocol of human bronchial epithelium in vitro to study the long-term effects of atmospheric particles. Toxicol. Vitro 27, 533–542.

Chen, Q., Wang, M., Wang, Y., Zhang, L., Li, Y., Han, Y., 2019. Oxidative potential of water-soluble matter associated with chromophoric substances in PM2.5 over Xi'an, China. Environ. Sci. Technol. 53, 8574–8584.

Chen, Q., Sun, H., Wang, M., Mu, Z., Wang, Y., Li, Y., Wang, Y., Zhang, L., Zhang, Z., 2018. Dominant fraction of EPFRs from nonsolvent-extractable organic matter in fine particulates over Xi'an, China. Environ. Sci. Technol. 52, 9646–9655.

Chowdhury, P.H., He, Q., Lasitza Male, T., Brune, W.H., Rudich, Y., Pardo, M., 2018. Exposure of lung epithelial cells to photochemically aged secondary organic aerosol shows increased toxic effects. Environ. Sci. Technol. Lett. 5, 424–430.

Chuang, H.-C., Shie, R.-H., Chio, C.-P., Yuan, T.-H., Lee, J.-H., Chan, C.-C., 2018. Cluster analysis of fine particulate matter (PM 2.5) emissions and its bioreactivity in the vicinity of a petrochemical complex. Environ. Pollut. 236, 591–597.

Chuang, H.-C., Sun, J., Ni, H., Tian, J., Lui, K.H., Han, Y., Cao, J., Huang, R.-J., Shen, Z., Ho, K.-F., 2019. Characterization of the chemical components and bioreactivity of fine particulate matter produced during crop-residue burning in China. Environ. Pollut. 245, 226–234.

Daher, N., Saliba, N.A., Shihadeh, A.L., Jaafar, M., Baalbaki, R., Shafer, M.M., Schauer, J.J., Sioutas, C., 2014. Oxidative potential and chemical speciation of size-resolved particulate matter (PM) at near-freeway and urban background sites in the greater Beirut area. Sci. Total Environ. 470, 417–426.

Delfino, R.J., Staimer, N., Tjoa, T., Arhami, M., Polidori, A., Gillen, D.L., George, S.C., Shafer, M.M., Schauer, J.J., Sioutas, C., 2010a. Associations of primary and secondary organic aerosols with airway and systemic inflammation in an elderly panel cohort. Epidemiology (Cambridge, Mass 21.

Delfino, R.J., Staimer, N., Tjoa, T., Arhami, M., Polidori, A., Gillen, D.L., Kleinman, M.T., Schauer, J.J., Sioutas, C., 2010b. Association of biomarkers of systemic inflammation with organic components and source tracers in quasi-ultrafine particles. Environ. Health Perspect. 118, 756–762.

Dergham, M., Lepers, C., Verdin, A., Billet, S., Cazier, F., Courcot, D., Shirali, P., Garçon, G., 2012. Prooxidant and proinflammatory potency of air pollution particulate matter (PM2.5–0.3) produced in rural, urban, or industrial surroundings in human bronchial epithelial cells (BEAS-2B). Chem. Res. Toxicol. 25, 904–919.

Dergham, M., Lepers, C., Verdin, A., Cazier, F., Billet, S., Courcot, D., Shirali, P., Garçon, G., 2015. Temporal–spatial variations of the physicochemical characteristics of air pollution particulate matter (PM2. 5–0.3) and toxicological effects in human bronchial epithelial cells (BEAS-2B). Environ. Res. 137, 256–267.

Dieme, D., Cabral-Ndior, M., Garçon, G., Verdin, A., Billet, S., Cazier, F., Courcot, D., Diouf, A., Shirali, P., 2012. Relationship between physicochemical characterization and toxicity of fine particulate matter (PM2. 5) collected in Dakar city (Senegal). Environ. Res. 113, 1–13.

Dinoi, A., Donateo, A., Belosi, F., et al., 2017. Comparison of atmospheric particle concentration measurements using different optical detectors: potentiality and limits for air quality applications. Measurement 106, 274–282.

Feng, J., Hu, M., Chan, C.K., Lau, P., Fang, M., He, L., Tang, X., 2006. A comparative study of the organic matter in PM2. 5 from three Chinese megacities in three different climatic zones. Atmos. Environ. 40, 3983–3994.

Feng, J., Sun, P., Hu, X., Zhao, W., Wu, M., Fu, J., 2012. The chemical composition and sources of PM2. 5 during the 2009 Chinese New Year's holiday in Shanghai. Atmos. Res. 118, 435–444.

Feng, S., Gao, D., Liao, F., Zhou, F., Wang, X., 2016. The health effects of ambient PM2. 5 and potential mechanisms. Ecotoxicol. Environ. Saf. 128, 67–74.

Fuentes-Mattei, E., Rivera, E., Gioda, A., Sanchez-Rivera, D., Roman-Velazquez, F.R., Jimenez-Velez, B.D., 2010. Use of human bronchial epithelial cells (BEAS-2B) to study immunological markers resulting from exposure to PM2. 5 organic extract from Puerto Rico. Toxicol. Appl. Pharmacol. 243, 381–389.

Gao, B., Guo, H., Wang, X.-M., Zhao, X.-Y., Ling, Z.-H., Zhang, Z., Liu, T.-Y., 2013. Tracer-based source apportionment of polycyclic aromatic hydrocarbons in PM 2.5 in Guangzhou, southern China, using positive matrix factorization (PMF). Environ. Sci. Pollut. Control Ser. 20, 2398–2409.

Gaschen, A., Lang, D., Kalberer, M., Savi, M., Geiser, T., Gazdhar, A., Lehr, C.-M., Bur, M., Dommen, J., Baltensperger, U., 2010. Cellular responses after exposure of lung cell cultures to secondary organic aerosol particles. Environ. Sci. Technol. 44, 1424–1430.

Gerde, P., Muggenburg, B.A., Lundborg, M., Dahl, A.R., 2001. The rapid alveolar

absorption of diesel soot-adsorbed benzo[a]pyrene: bioavailability, metabolism and dosimetry of an inhaled particle-borne carcinogen. Carcinogenesis 22, 741–749.
Happo, M., Markkanen, A., Markkanen, P., Jalava, P., Kuuspalo, K., Leskinen, A., Sippula, O., Lehtinen, K., Jokiniemi, J., Hirvonen, M.-R., 2013. Seasonal variation in the toxicological properties of size-segregated indoor and outdoor air particulate matter. Toxicol. Vitro 27, 1550–1561.
He, L.-Y., Hu, M., Huang, X.-F., Zhang, Y.-H., Tang, X.-Y., 2006. Seasonal pollution characteristics of organic compounds in atmospheric fine particles in Beijing. Sci. Total Environ. 359, 167–176.
Ho, K.-F., Chang, C.-C., Tian, L., Chan, C.-S., Musa Bandowe, B.A., Lui, K.-H., Lee, K.-Y., Chuang, K.-J., Liu, C.-Y., Ning, Z., Chuang, H.-C., 2016. Effects of polycyclic aromatic compounds in fine particulate matter generated from household coal combustion on response to EGFR mutations in vitro. Environ. Pollut. 218, 1262–1269.
Ho, S.S.H., Chow, J.C., Watson, J.G., Ting Ng, L.P., Kwok, Y., Ho, K.F., Cao, J., 2011. Precautions for in-injection port thermal desorption-gas chromatography/mass spectrometry (TD-GC/MS) as applied to aerosol filter samples. Atmos. Environ. 45, 1491–1496.
Ho, S.S.H., Yu, J.Z., 2004. In-injection port thermal desorption and subsequent gas chromatography–mass spectrometric analysis of polycyclic aromatic hydrocarbons and n-alkanes in atmospheric aerosol samples. J. Chromatogr. A 1059, 121–129.
Huang, X.-F., He, L.-Y., Hu, M., Zhang, Y.-H., 2006. Annual variation of particulate organic compounds in PM2. 5 in the urban atmosphere of Beijing. Atmos. Environ. 40, 2449–2458.
Jia, Y.-Y., Wang, Q., Liu, T., 2017. Toxicity research of PM2. 5 compositions in vitro. Int. J. Environ. Res. Publ. Health 14, 232.
Jomova, K., Valko, M., 2011. Advances in metal-induced oxidative stress and human disease. Toxicology 283, 65–87.
Kim, K.-H., Kabir, E., Kabir, S., 2015. A review on the human health impact of airborne particulate matter. Environ. Int. 74, 136–143.
Künzi, L., Mertes, P., Schneider, S., Jeannet, N., Menzi, C., Dommen, J., Baltensperger, U., Prévôt, A.S., Salathe, M., Kalberer, M., 2013. Responses of lung cells to realistic exposure of primary and aged carbonaceous aerosols. Atmos. Environ. 68, 143–150.
Lanz, V., Prévôt, A., Alfarra, M., Weimer, S., Mohr, C., DeCarlo, P., Gianini, M., Hueglin, C., Schneider, J., Favez, O., 2010. Characterization of aerosol chemical composition with aerosol mass spectrometry in Central Europe: an overview. Atmos. Chem. Phys. 10, 10453.
Lionetto, M.G., Guascito, M.R., Caricato, R., Giordano, M.E., De Bartolomeo, A.R., Romano, M.P., Conte, M., Dinoi, A., Contini, D., 2019. Correlation of oxidative potential with ecotoxicological and cytotoxicological potential of PM10 at an urban background site in Italy. Atmosphere 10, 733.
Li, Y., Lee, B., Su, L., Fung, J.C., Chan, C., 2015. Seasonal characteristics of fine particulate matter (PM) based on high-resolution time-of-flight aerosol mass spectrometric (HR-ToF-AMS) measurements at the HKUST Supersite in Hong Kong. Atmos. Chem. Phys. 15, 37–53.
Li, Y., Lee, B., Yu, J., Ng, N., Chan, C., 2013. Evaluating the degree of oxygenation of organic aerosol during foggy and hazy days in Hong Kong using high-resolution time-of-flight aerosol mass spectrometry (HR-ToF-AMS). Atmos. Chem. Phys. Discuss. 13.
Lin, Y.-H., Arashiro, M., Martin, E., Chen, Y., Zhang, Z., Sexton, K.G., Gold, A., Jaspers, I., Fry, R.C., Surratt, J.D., 2016. Isoprene-derived secondary organic aerosol induces the expression of oxidative stress response genes in human lung cells. Environ. Sci. Technol. Lett. 3, 250–254.
Liu, Y., Chen, Y.-Y., Cao, J.-Y., Tao, F.-B., Zhu, X.-X., Yao, C.-J., Chen, D.-J., Che, Z., Zhao, Q.-H., Wen, L.-P., 2015. Oxidative stress, apoptosis, and cell cycle arrest are induced in primary fetal alveolar type II epithelial cells exposed to fine particulate matter from cooking oil fumes. Environ. Sci. Pollut. Control Ser. 22, 9728–9741.
Longhin, E., Holme, J.A., Gutzkow, K.B., Arlt, V.M., Kucab, J.E., Camatini, M., Gualtieri, M., 2013a. Cell cycle alterations induced by urban PM2. 5 in bronchial epithelial cells: characterization of the process and possible mechanisms involved. Part. Fibre Toxicol. 10, 63.
Longhin, E., Pezzolato, E., Mantecca, P., Holme, J., Franzetti, A., Camatini, M., Gualtieri, M., 2013b. Season linked responses to fine and quasi-ultrafine Milan PM in cultured cells. Toxicol. Vitro 27, 551–559.
Lonkar, P., Dedon, P.C., 2011. Reactive species and DNA damage in chronic inflammation: reconciling chemical mechanisms and biological fates. Int. J. Canc. 128, 1999–2009.
Louie, P.K., Watson, J.G., Chow, J.C., Chen, A., Sin, D.W., Lau, A.K., 2005. Seasonal characteristics and regional transport of PM2. 5 in Hong Kong. Atmos. Environ. 39, 1695–1710.
Lui, K., Bandowe, B.A.M., Ho, S.S.H., Chuang, H.-C., Cao, J.-J., Chuang, K.-J., Lee, S., Hu, D., Ho, K., 2016. Characterization of chemical components and bioreactivity of fine particulate matter (PM2. 5) during incense burning. Environ. Pollut. 213, 524–532.
Middlebrook, A.M., Bahreini, R., Jimenez, J.L., Canagaratna, M.R., 2012. Evaluation of composition-dependent collection efficiencies for the aerodyne aerosol mass spectrometer using field data. Aerosol. Sci. Technol. 46, 258–271.
Mikuška, P., Křůmal, K., Večeřa, Z., 2015. Characterization of organic compounds in the PM2. 5 aerosols in winter in an industrial urban area. Atmos. Environ. 105, 97–108.
Naimabadi, A., Ghadiri, A., Idani, E., Babaei, A.A., Alavi, N., Shirmardi, M., Khodadadi, A., Marzouni, M.B., Ankali, K.A., Rouhizadeh, A., Goudarzi, G., 2016. Chemical composition of PM10 and its in vitro toxicological impacts on lung cells during the Middle Eastern Dust (MED) storms in Ahvaz, Iran. Environ. Pollut. 211, 316–324.
Ng, N.L., Herndon, S.C., Trimborn, A., Canagaratna, M.R., Croteau, P., Onasch, T.B., Sueper, D., Worsnop, D.R., Zhang, Q., Sun, Y., 2011. An Aerosol Chemical Speciation Monitor (ACSM) for routine monitoring of the composition and mass concentrations of ambient aerosol. Aerosol. Sci. Technol. 45, 780–794.
Nielsen, T., 1996. Traffic contribution of polycyclic aromatic hydrocarbons in the center of a large city. Atmos. Environ. 30, 3481–3490.
Nordin, E.Z., Uski, O., Nyström, R., Jalava, P., Eriksson, A.C., Genberg, J., Roldin, P., Bergvall, C., Westerholm, R., Jokiniemi, J., 2015. Influence of ozone initiated processing on the toxicity of aerosol particles from small scale wood combustion. Atmos. Environ. 102, 282–289.
Oh, S.M., Kim, H.R., Park, Y.J., Lee, S.Y., Chung, K.H., 2011. Organic extracts of urban air pollution particulate matter (PM2. 5)-induced genotoxicity and oxidative stress in human lung bronchial epithelial cells (BEAS-2B cells). Mutat. Res. Genet. Toxicol. Environ. Mutagen 723, 142–151.
Ovrevik, J., Arlt, V.M., Oya, E., Nagy, E., Mollerup, S., Phillips, D.H., Lag, M., Holme, J.A., 2010. Differential effects of nitro-PAHs and amino-PAHs on cytokine and chemokine responses in human bronchial epithelial BEAS-2B cells. Toxicol. Appl. Pharmacol. 242, 270–280.
Paatero, P., 1997. Least squares formulation of robust non-negative factor analysis. Chemometr. Intell. Lab. Syst. 37, 23–35.
Paatero, P., Tapper, U., 1994. Positive matrix factorization: a non-negative factor model with optimal utilization of error estimates of data values. Environmetrics 5, 111–126.
Perrone, M., Gualtieri, M., Consonni, V., Ferrero, L., Sangiorgi, G., Longhin, E., Ballabio, D., Bolzacchini, E., Camatini, M., 2013. Particle size, chemical composition, seasons of the year and urban, rural or remote site origins as determinants of biological effects of particulate matter on pulmonary cells. Environ. Pollut. 176, 215–227.
Riedl, M., Diaz-Sanchez, D., 2005. Biology of diesel exhaust effects on respiratory function. J. Allergy Clin. Immunol. 115, 221–228.
Riva, D., Magalhaes, C., Lopes, A.A., Lancas, T., Mauad, T., Malm, O., Valenca, S., Saldiva, P., Faffe, D., Zin, W., 2011. Low dose of fine particulate matter (PM2. 5) can induce acute oxidative stress, inflammation and pulmonary impairment in healthy mice. Inhal. Toxicol. 23, 257–267.
Rogge, W.F., Hildemann, L.M., Mazurek, M.A., Cass, G.R., Simoneit, B.R.T., 1991. Sources of fine organic aerosol. 1. Charbroilers and meat cooking operations. Environ. Sci. Technol. 25, 1112–1125.
Simoneit, B.R., Cox, R., Standley, L., 1988. Organic matter of the troposphere—IV. Lipids in Harmattan aerosols of Nigeria. Atmos. Environ. 22, 983–1004, 1967.
Simoneit, B.R.T., Mazurek, M.A., 1982. Organic matter of the troposphere—II.**For Part I, see Simoneit et al. (1977). Natural background of biogenic lipid matter in aerosols over the rural western United States. Atmos. Environ. 16, 2139–2159, 1967.
Sun, C., Lee, B., Huang, D., Jie Li, Y., Schurman, M., Louie, P., Luk, C., Chan, C., 2016. Continuous measurements at the urban roadside in an Asian megacity by Aerosol Chemical Speciation Monitor (ACSM): particulate matter characteristics during fall and winter seasons in Hong Kong. Atmos. Chem. Phys. 16, 1713–1728.
Sun, J., Shen, Z., Zeng, Y., Niu, X., Wang, J., Cao, J., Gong, X., Xu, H., Wang, T., Liu, H., 2018. Characterization and cytotoxicity of PAHs in PM 2.5 emitted from residential solid fuel burning in the Guanzhong Plain, China. Environ. Pollut. 241, 359–368.
Sun, J., Zhang, Q., Canagaratna, M.R., Zhang, Y., Ng, N.L., Sun, Y., Jayne, J.T., Zhang, X., Zhang, X., Worsnop, D.R., 2010. Highly time-and size-resolved characterization of submicron aerosol particles in Beijing using an Aerodyne Aerosol Mass Spectrometer. Atmos. Environ. 44, 131–140.
Sun, Y., Wang, Z., Fu, P., Yang, T., Jiang, Q., Dong, H., Li, J., Jia, J., 2013. Aerosol composition, sources and processes during wintertime in Beijing, China. Atmos. Chem. Phys. 13, 4577–4592.
Terzano, C., Di Stefano, F., Conti, V., Graziani, E., Petroianni, A., 2010. Air pollution ultrafine particles: toxicity beyond the lung. Eur. Rev. Med. Pharmacol. Sci. 14, 809–821.
Velali, E., Papachristou, E., Pantazaki, A., Choli-Papadopoulou, T., Argyrou, N., Tsourouktsoglou, T., Lialiaris, S., Constantinidis, A., Lykidis, D., Lialiaris, T.S., Besis, A., Voutsa, D., Samara, C., 2016. Cytotoxicity and genotoxicity induced in vitro by solvent-extractable organic matter of size-segregated urban particulate matter. Environ. Pollut. 218, 1350–1362.
Wang, Y., Wang, M., Li, S., Sun, H., Mu, Z., Zhang, L., Li, Y., Chen, Q., 2020. Study on the oxidation potential of the water-soluble components of ambient PM2.5 over Xi'an, China: pollution levels, source apportionment and transport pathways. Environ. Int. 136, 105515.
Wang, J., Ho, S.S.H., Ma, S., Cao, J., Dai, W., Liu, S., Shen, Z., Huang, R., Wang, G., Han, Y., 2016. Characterization of PM2. 5 in Guangzhou, China: uses of organic markers for supporting source apportionment. Sci. Total Environ. 550, 961–971.
Wu, D., Zhang, F., Lou, W.H., Li, D., Chen, J.M., 2017. Chemical characterization and toxicity assessment of fine particulate matters emitted from the combustion of petrol and diesel fuels. Sci. Total Environ. 605, 172–179.
Xu, F., Qiu, X., Hu, X., Shang, Y., Pardo, M., Fang, Y., Wang, J., Rudich, Y., Zhu, T., 2018. Effects on IL-1β signaling activation induced by water and organic extracts of fine particulate matter (PM2. 5) in vitro. Environ. Pollut. 237, 592–600.
Xu, H.M., Ho, S.S.H., Gao, M.L., Cao, J.J., Guinot, B., Ho, K.F., Long, X., Wang, J.Z.,

Shen, Z.X., Liu, S.X., Zheng, C.L., Zhang, Q., 2016. Microscale spatial distribution and health assessment of PM2.5-bound polycyclic aromatic hydrocarbons (PAHs) at nine communities in Xi'an, China. Environ. Pollut. 218, 1065–1073.
Yang, H., Yu, J.Z., Ho, S.S.H., Xu, J., Wu, W.-S., Wan, C.H., Wang, X., Wang, X., Wang, L., 2005. The chemical composition of inorganic and carbonaceous materials in PM2. 5 in Nanjing, China. Atmos. Environ. 39, 3735–3749.
Zhang, Y., Sheesley, R.J., Schauer, J.J., Lewandowski, M., Jaoui, M., Offenberg, J.H., Kleindienst, T.E., Edney, E.O., 2009. Source apportionment of primary and secondary organic aerosols using positive matrix factorization (PMF) of molecular markers. Atmos. Environ. 43, 5567–5574.
Zou, Y., Jin, C., Su, Y., Li, J., Zhu, B., 2016. Water soluble and insoluble components of urban PM2. 5 and their cytotoxic effects on epithelial cells (A549) in vitro. Environ. Pollut. 212, 627–635.